Acta Biochimica Polonica

Vol. 48 No. 1/2001

65–75

QUARTERLY

The effect of the Glu342Lys mutation in α_1-antitrypsin on its structure, studied by molecular modelling methods★⋆✪

Grzegorz Jezierski✉ and Marta Pasenkiewicz-Gierula

Biophysics Department, Institute of Molecular Biology, Jagiellonian University, Kraków, Poland

Received: 8 January, 2001; revised: 26 January, 2001; accepted: 6 February, 2001

Key words: molecular dynamics simulation, energy minimisation, serpins, protein structure

The structure of native α_1-antitrypsin, the most abundant protease inhibitor in human plasma, is characterised primarily by a reactive loop containing the centre of proteinase inhibition, and a β-sheet composed of five strands. Mobility of the reactive loop is confined as a result of electrostatic interactions between side chains of Glu342 and Lys290, both located at the junction of the reactive loop and the β structure. The most common mutation in the protein, resulting in its inactivation, is Glu342→Lys, named the Z mutation.

The main goal of this work was to investigate the influence of the Z mutation on the structure of α_1-antitrypsin. Commonly used molecular modelling methods have been applied in a comparative study of two protein models: the wild type and the Z mutant.

The results indicate that the Z mutation introduces local instabilities in the region of the reactive loop. Moreover, even parts of the protein located far apart from the mutation region are affected. The Z mutation causes a relative change in the total energy of about 3%. Relatively small root mean square differences between the optimised structures of the wild type and the Z mutant, together with detailed analysis of 'conformational searching' process, lead to the hypothesis that the Z mutation principally induces a change in the dynamics of α_1-antitrypsin.

Human α_1-antitrypsin is a serine proteinase inhibitor belonging to the group of serpins [1, 2]. It is the most abundant protease inhibitor in human plasma, and is widely investigated at present [3–6]. Structural features characteristic of serpins and crucial for biological function of α_1-antitrypsin include:

- a reactive loop, exposed to solvent and containing the centre of proteinase inhibition (see Fig. 1),

★Presented at the International Conference on "Conformation of Peptides, Proteins and Nucleic Acids", Debrzyno, Poland, 2000.

⋆The calculations were performed at the Interdisciplinary Centre for Mathematical Modelling, Warsaw, Poland, on Cray T3E 'Tsunami'.

✪This work has been supported by the State Committee for Scientific Research (KBN); grant no. 4 P05A 081 14.

✉Corresponding author: Grzegorz Jezierski, Institute of Molecular Biology, al. A. Mickiewicza 3, 31-120 Kraków, Poland; phone: (12) 6341305, ext. 291, fax: 6336907, e-mail: gj@mol.uj.edu.pl

Abbreviations: AMBER, assisted model building for energy refinement; MD, molecular dynamics; FFT, fast Fourier transform; NMR, nuclear magnetic resonance; OPLS, optimized potentials for liquid simulations; r.m.s., root mean square; r.m.s.d., root mean square displacement.

- a large A sheet consisting of 5 β-strands (see Fig. 6a),
- a small C sheet consisting of 4 β-strands and linked strictly to the A sheet (see Fig. 1).

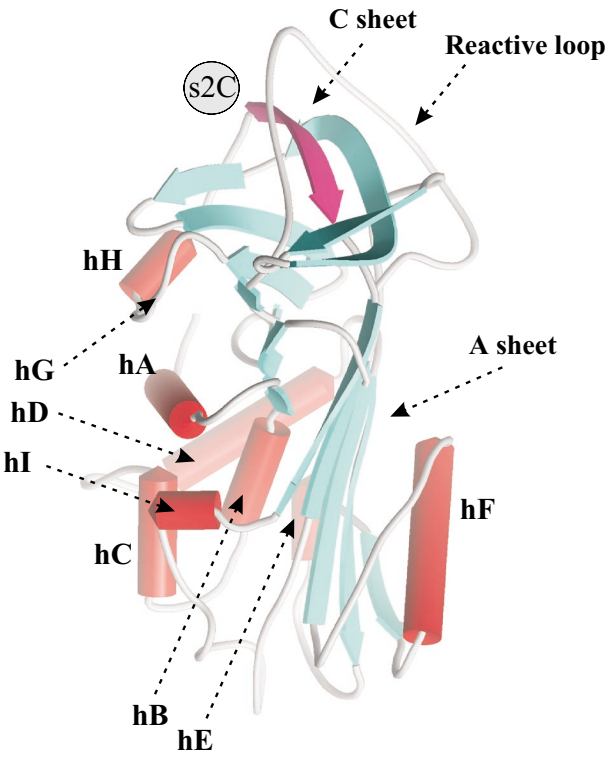

Figure 1. Secondary structure of α_1-antitrypsin in its native form [8].

The picture shows α-helical (red cylinders) and β-structured (blue ribbons) fragments of the polypeptide chain. The model was oriented so that all helices are visible. There are nine helices, denoted hA, hB,..., hH; the G helix is not shown as a cylinder but is indicated by an arrow. The β-sheet situated on the right-hand side of the model, in vertical position, is identified as 'A sheet'. A small β-sheet, identified as 'C sheet', is visible at the top of the model. It contains strand No. 2, denoted s2C, which is coloured magenta.

Mobility of the reactive loop is confined as a result of electrostatic interactions between side chains of Glu342 and Lys290, both located at the junction of the reactive loop and the β structure (see Fig. 6b). α_1-Antitrypsin can adopt several structural forms that differ mainly by conformation of the reactive loop. One of them is the native form, which is able to inhibit proteinases and which circulates in human plasma. Another is the cleaved form, with a cleaved peptide bond on the reactive loop and a part of the loop inserted to the A sheet as a β-strand. Upon proteolytic cleavage in the centre of inhibition or in its vicinity, the reactive loop is broken into two strands; one of them is incorporated into the five-stranded β-sheet, thus forming a six-stranded β-sheet [7]. Three-dimensional structures of these two forms were determined by X-ray diffraction [7, 8].

Numerous genetic variants of α_1-antitrypsin have been identified; many of them undergo spontaneous polymerisation, leading to retention of the protein within hepatocytes and, in consequence, to a decrease in its concentration in plasma. This phenomenon causes several diseases, most notably emphysema and liver cirrhosis [9–12]. The most common variant of α_1-antitrypsin, Glu342→Lys, named the Z variant or – as in this paper – the Z mutant, is known to polymerise *in vivo* [13] but has also been shown to polymerise spontaneously *in vitro* [14]. The structural changes involved in polymerisation are not known, although two crystal structures of polymerised α_1-antitrypsin in its cleaved forms have been reported [15, 16]. Based on these structures, and on other experimental data [17] it is commonly assumed that the Z mutant polymerises by insertion of a part of its reactive loop to the A sheet of another molecule. In this way, self-repeated units assemble into linear or circular polymers. However, much evidence exists for another mechanism of α_1-antitrypsin polymerisation, in which the reactive loop interacts with the C sheet of another molecule. Polymers of this type are induced by sodium citrate or result from the point mutation ΔPhe52 [18, 19].

Investigation of Glu342→Lys mutation in terms of conformation of α_1-antitrypsin is important for understanding the mechanism of its polymerisation. Application of computational techniques such as simulated annealing and energy minimisation is, according to the authors of this paper, justified by complementarity of these methods to other methods of structural analysis (e.g. X-ray diffraction, fluorometric methods).

METHODS

The study comprised three stages: construction of a model of the mutant, a protocol of 'sequential' simulated annealing, and energy minimisation of structures obtained sequentially during the course of simulation. Identical procedures were carried out for the mutant and the wild type protein models.

1. The model of the Z mutant was constructed based on the structure of α_1-antitrypsin in its native (uncleaved) form [7]. The obtained structure was minimised using the 'steepest descents' and then the 'conjugate gradients' algorithm; 5 000 iterations were calculated with each algorithm.

2. Each model was then subjected to a simulated annealing protocol. The protocol included molecular dynamics (MD) simulation with temperature changes (see Fig. 2). The temperature was increased linearly from 10 K to 500 K during the first 10 ps of the simulation. The resulting structure was simulated at 500 K for 10 ps (high temperature MD) and then the temperature was decreased exponentially to 310 K during 40 ps ('cooling'). The protocol of a high temperature MD and cooling was repeated 20 times, starting from structures after 10, 20, 30, etc. ps of the high temperature MD. This yielded 20 structures for each of the two models.

3. Each of the 20 structures for each model was optimised. For further studies, the structure of the lowest energy and the lowest r.m.s. fluctuation values was selected for each model. The selected structures were those after 170 ps (structure no. 17) of the high temperature MD for the wild type, and 140 ps (structure No. 14) – for the mutant.

The protein was simulated with the OPLS *united atom* force field [20]. In all simulations reported here the cutoff radius was 12.0 Å. Distance dependent dielectric 'constant' equal to 1.0 r was used in order to account for solvent screening effects. It was assumed that including of explicit solvent could destabilise the protein structure at 500 K, as a significant part of the polypeptide chain was restrained with a flat-bottomed potential (see below).

The algorithms for energy minimisation were 'steepest descents', and then 'conjugate gradients' – 10 000 iterations were calculated with each algorithm. These algorithms do not become unstable when a structure is far from minimum, therefore they are suitable for coarse minimisation of large structures having many possible metastable conformations, e.g. proteins. No other algorithm was applied as we did not intend to obtain a completely refined structure.

During simulated annealing procedure the SHAKE [21] algorithm was applied for bonds involving hydrogen, and 1 fs time step was used. Constant temperature was controlled using the algorithm of Berendsen [22].

During simulated annealing, dihedral angles within the protein backbone were restrained with soft parabolic-linear potential. For helical and β-sheet fragments, the potential well was parabolic within $\phi \pm \pi$ rad around an actual dihedral angle. For the remaining fragments, the potential value was equal to zero within $\phi \pm (\pi/2)$ rad and the potential well was parabolic outside this range. For both potentials, the force constant was equal to 600 kcal/(mol*rad^2), and for angles exceeding $\phi \pm \pi$, the potential values were scaled linearly with ϕ. These restraints were applied to prevent regions with clearly defined secondary structure from significant unfolding at high temperature. The restraints were imposed as implemented in AMBER [23]. The parameters were obtained based on procedures of structure determination by NMR and simulated annealing protocols [24, 25], as well as on tests performed by G.J. on a model tripeptide (to be published later).

Construction of the model (stage 1), visualisation procedures and protein drawings were made using MSI software: InsightII (ver. 97.0) and WebLab ViewerLite (ver. 3.5) [26]. Molecular dynamics simulations, energy minimisation and most of data analysis were performed using the AMBER software package (ver. 4.1) [23]. For comparative analyses of secondary structure, diagrams produced by DSSP program [27] were used. DSSP was developed by Kabsch and Sander, based on their classification of secondary structures of proteins.

RESULTS AND DISCUSSION

Preliminary remarks

The goals of calculations described in this paper were:

1. Analysis of conformational changes in the Z mutant of α_1-antitrypsin, during high temperature simulation, relative to changes in the wild type.

2. Generation of a model of the Z mutant, which would serve as a starting structure for further simulations.

It has been assumed that the optimal protocol of simulation in this time scale is to generate an MD trajectory at high temperature and several trajectories at temperatures decreasing from 500 K to the physiological temperature. A plot of the systems temperature during generation of an ensemble of structures is shown in Fig. 2.

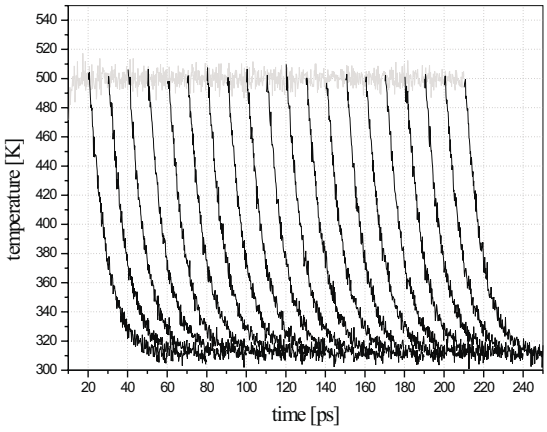

Figure 2. Plot of temperature *vs* time in simulated annealing protocol of α_1-antitrypsin.

The protocol consists of increasing temperature from 10 K to 500 K (not shown here) during 10 ps of the simulation, high temperature MD simulation at 500 K for 200 ps (light gray line) and exponential 'cooling' of momentary structures obtained every 10 ps of high temperature MD simulation to 310 K during 40 ps (black lines).

In this paper, the structures generated during MD simulation are referred to as 'dynamical structures' ('not cooled'); and the structures obtained as a result of cooling and subsequent energy minimisation are referred to as 'optimised structures'.

Changes in energy values during simulated annealing

Time profiles of the total energy for two models: the wild type and the Z mutant have been analysed. Plots of the system's energy *vs* simulation time (Fig. 3) show, during the first 10 ps of MD simulation at 500 K, a peak diffused towards greater values of time. It is an effect of relatively rapid, linear heating of the system. Between 20 ps and 40 ps, the decrease of the energy mean values becomes slower, corresponding to energy stabilisation. Energy of the wild type model is stabilised more rapidly, reaching the level of 1750 kcal/mol within the first 60 ps of high temperature MD simulation. At 60 ps, the total energy value for the mutant is by 100 kcal/mol higher than for the wild type and exhibits a higher amplitude of fluctuations. The periods of energy fluctuations are similar in the two models; perhaps this is an effect of the same coupling constant to a heat bath.

Selected elements of 'dynamical' structure

Figure 5 shows distances between residues No. 342 (glutamic acid in the wild type; lysine in the mutant) and 290 (lysine) *vs* simulation time. The distance between the carboxylic carbon of Glu342 and ζ nitrogen of Lys290 remains stable throughout the run and its average value is 3.18 ± 0.19 Å, whereas the distance between the two ζ nitrogens of the corresponding residues in the Z mutant undergoes large variations, its average value being 10.74 ± 1.08 Å. In the mutant, the break-up of stable interaction between residues No. 342 and 290 causes separation of the backbone carbon atoms by 2 Å more.

Conformational variations between 'dynamical' structures are clearly visible after superimposing these structures for the mutant and the wild type. Five representative 'dynamical' structures are compared in Fig. 5. Most notably, distortion of a 'hinge' of the reactive loop is smaller in the wild type than in the mutant. One may also observe that in the mutant, amino-acid side chains at the inhibition centre (often denoted P1–P1′) are less exposed to solvent than in the wild type. Superimposed 'dynamical' structures of the reactive loop show a higher relative conformational divergence

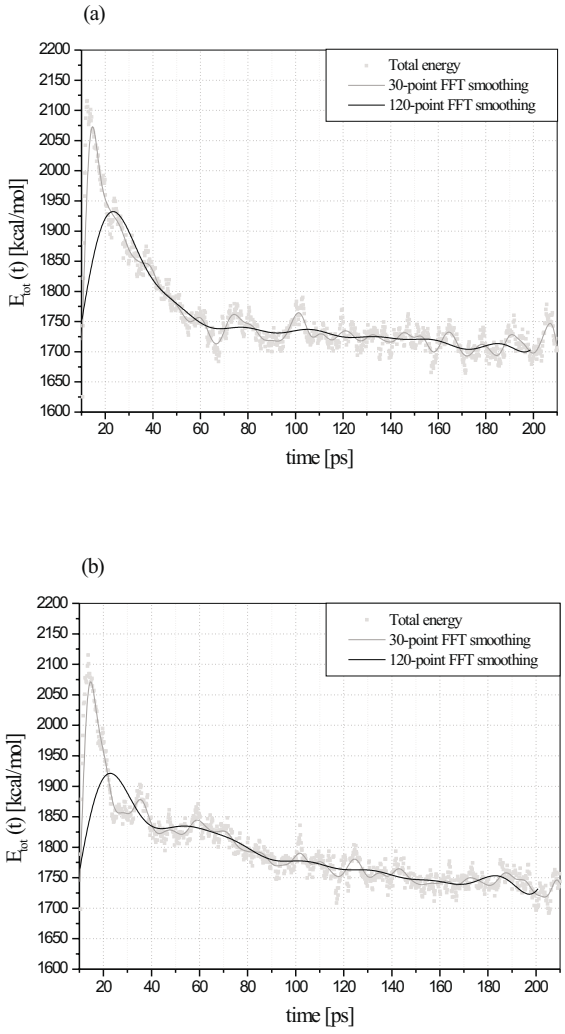

Figure 3. Plots of the total energy (E_{tot}) *vs* time in the simulated annealing protocol of α_1-antitrypsin, during MD simulation at 500 K.

Plots for the wild type (a) and the Z mutant (b) are shown for comparison. The total energy curves (scatter plot, light grey) smoothed by fast Fourier transform are shown (solid lines). The smoothing is accomplished by removing Fourier components with frequencies higher than 1/(n*Öt) where n is the number of data points considered at a time, and Öt is the time (or more generally the abscissa) spacing between two adjacent data points. The function used to clip out the high-frequency components is a parabola with its maximum of 1 at zero frequency and falling to zero at the cutoff frequency defined above. The parameters of this parabolic clipping function are determined by the total number of points and the number of points considered at one time. The more points are considered at a time, the greater is the degree of smoothing. 30-Point FFT smoothing (grey line) illustrates a period of energy fluctuations, here about 10 ps for both models. 120-Point FFT smoothing (black line) represents approximately the running average of energy values during the simulation.

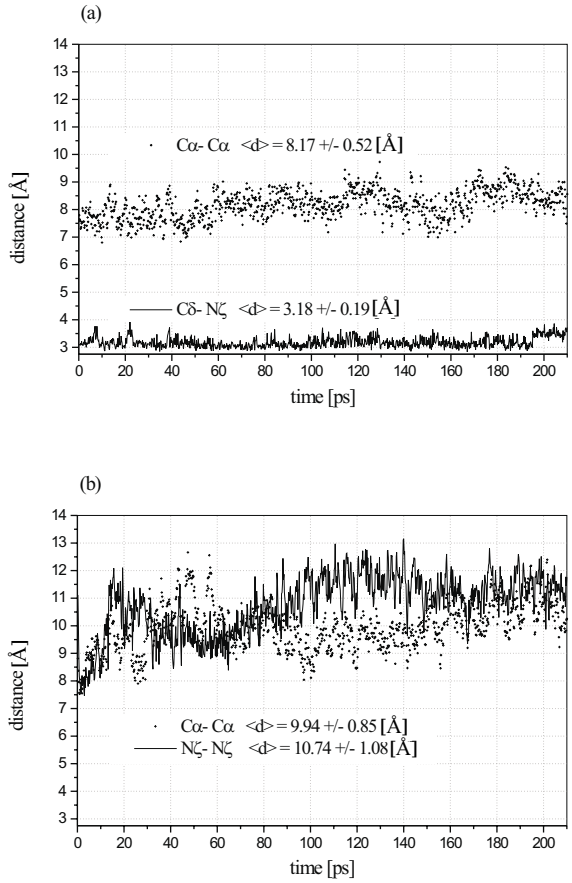

Figure 4. Plots of distances *vs* time between atoms in residues No. 342 and 290 in the wild type (a) and the Z mutant (b) of α_1-antitrypsin.

Here are shown distances during the high temperature MD simulation at 500 K (see Methods) between side-chain (scatter plot) and backbone C_α atoms (black line). Mean values of distances with standard errors are given.

as compared to the wild type. Interestingly, the latter observation is not confirmed by root mean square (r.m.s.) values of the best fit (quantitative measurement of similarity of superimposed 'dynamical' structures). The r.m.s. values vary from 1.34 Å to 2.57 Å for the wild type model and from 1.23 Å to 2.33 Å for the mutant model (see Table 1). This may be due to the way the values were calculated, i.e. strands no. 3A, 4A, 5A and 6A were taken together into account.

Secondary structure variation of 'dynamical' models

Due to limited MD simulation time, major changes in conformation of the models, e.g. ter-

tiary structure transformation, could not be observed. However, local changes in secondary structure could be expected. Secondary structures of the wild type and the Z mutant of α_1-antitrypsin during high temperature MD were compared in diagrams based on Kabsch and Sander classification. In this paper, only the most important observations are presented (both complete diagrams and their detailed analysis will be published elsewhere). 'Dynamical' structures of the wild type and the Z mutant, obtained in 140th ps of high temperature MD, were analysed. They were compared both to each other and to the optimised structure of the wild type that had been used as a starting model for simulated annealing.

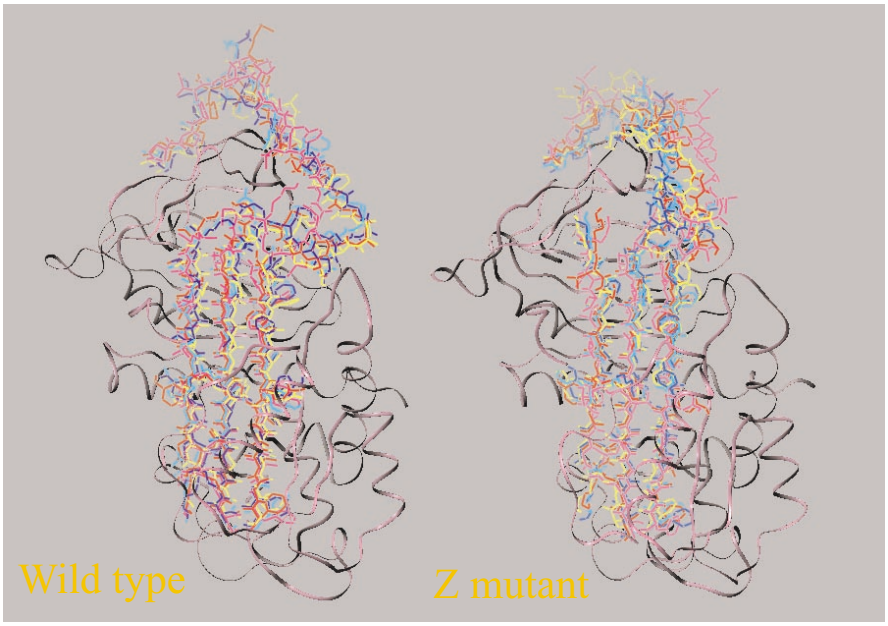

Figure 5. Comparison of two graphical representations of α_1-antitrypsin, the wild type and the Z mutant.

Strands No. 3, 4, 5 and 6 of the β-sheet A are presented in the form of 'dynamical' structures (line representation); the backbone of the rest of the molecule is represented by a ribbon. Five 'snapshots' taken during the high temperature MD at 500 K were superimposed (each is shown in a different colour). r.m.s. function for each pair of structures was minimised, and only the backbone depicted in line representation was taken into account during minimisation.

The latter model is referred to as 'the reference structure'.

There were only minor changes in the fragment connecting the F helix to strand s3A. Most notably, a 3-turn[1] absent in the reference structure appeared in the wild type model. This is the chain linking the upper part of the F helix with the A sheet, as seen in Fig. 1. The fragment connecting the strands s3A and s4C, situated at the junction of the A and C sheets, as well as in the proximity of the 'hinge' region (Fig. 6a), exhibits a 6-residue 'extended' structure in the wild type and a short bend in the mutant. Remarkably, identical features are formed for either variant, modelled by optimised structures (see analogous analysis below). In the fragment comprising Lys290, only minor changes in secondary structure have been identified in the diagram. Changes are slightly larger in a portion of strand s5A comprising Lys342 (mutant), where the length of a bend decreases. Conformational transition is also observed for the fragment connecting the leftmost strand of the A sheet (as seen in Fig. 6a) with the I helix. Here, an about 10-residue long fragment identified in the diagram to be an 'H-bonded turn' appears in the Z mutant in place of a turn and a helical structure in the wild type.

[1]A turn having 3 consecutive residues bracketed by an H-bond.

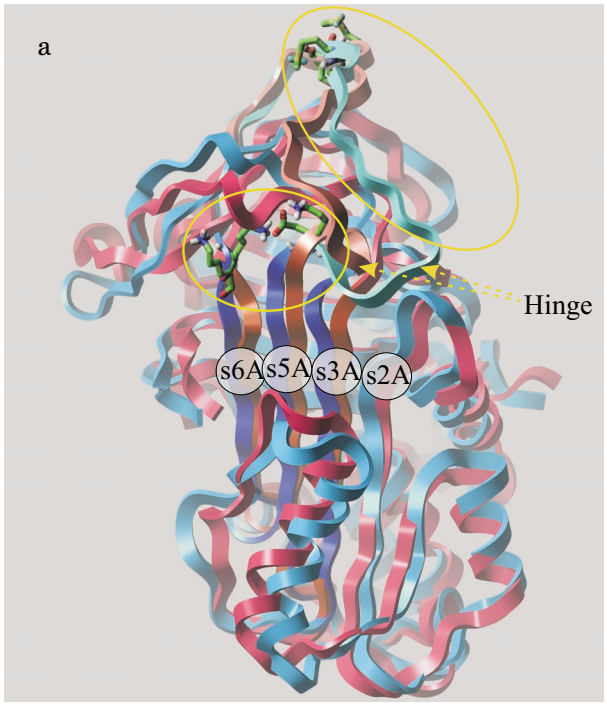

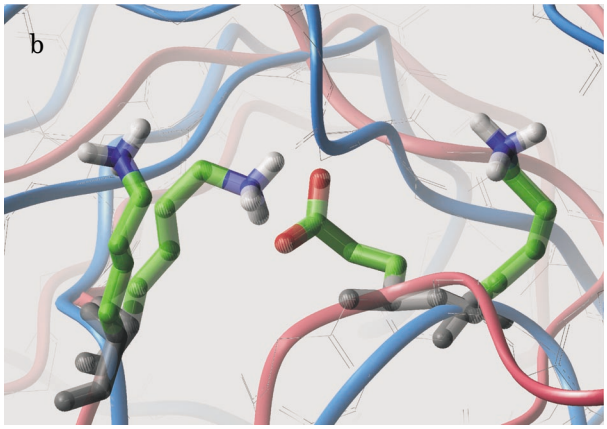

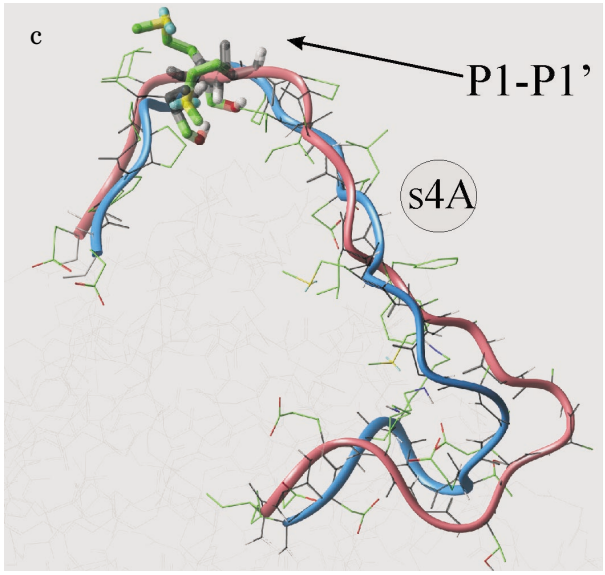

Figure 6. Graphical representation of two models of α_1-antitrypsin: the Z mutant and the wild type.

(a) Two optimised structures, those of the wild type (red ribbon) and of the Z mutant (blue ribbon) were superimposed. The five-stranded β-sheet is visible in front, and the reactive loop (lighter colours) at the top. Strands 3A, 5A, and 6A are labelled (in black circles). A 'hinge region', located at the junction of the β-sheet A and the reactive loop, is indicated by dashed arrows. Fragments of the model shown in detail in (b) and (c) are in orange ellipses. (b) A close-up of residues 342 and 290 is shown. The residues are in stick representation and are coloured by atom types. Residues Glu342 and Lys290 in the wild type protein form a stable electrostatic interaction, which does not exist in the mutant. (c) The picture shows the reactive loop (strand A4) of the two models, with the centre of proteolytic cleavage (Met358 and Ser359) in stick representation.

Conformational divergence of optimised structures

In order to choose a model structure of the Z mutant from a set of structures, energy minimisation was carried out after the simulated annealing procedure. It was assumed that, within a relatively small fragment of the conformational space, the most stable structure best approximates the native protein structure. This means that the criteria for choosing a 'proper' structure from a set of 20 were the lowest values of the total energy and the root mean square error of energy minimisation. The largest variations of final values of the total energy were 4% of its value in the wild type, which is 773 kcal/mol, and 2.3% in the mutant, which is 432 kcal/mol.

To illustrate how effectively the simulations penetrate conformational space, analysis of relative divergence between each of the 'optimised' structures was necessary. The divergence was measured by root mean square distance (r.m.s.d.), a parameter determined separately for two sets of atoms – one in the mutant and the other in the wild type. r.m.s.d. values were presented in the form of a matrix (see Fig. 7a–d), each position corresponding to one of the optimised structures. If a given structure is characterised by relatively large r.m.s.d. values with respect to other structures, this means the system has occupied, during

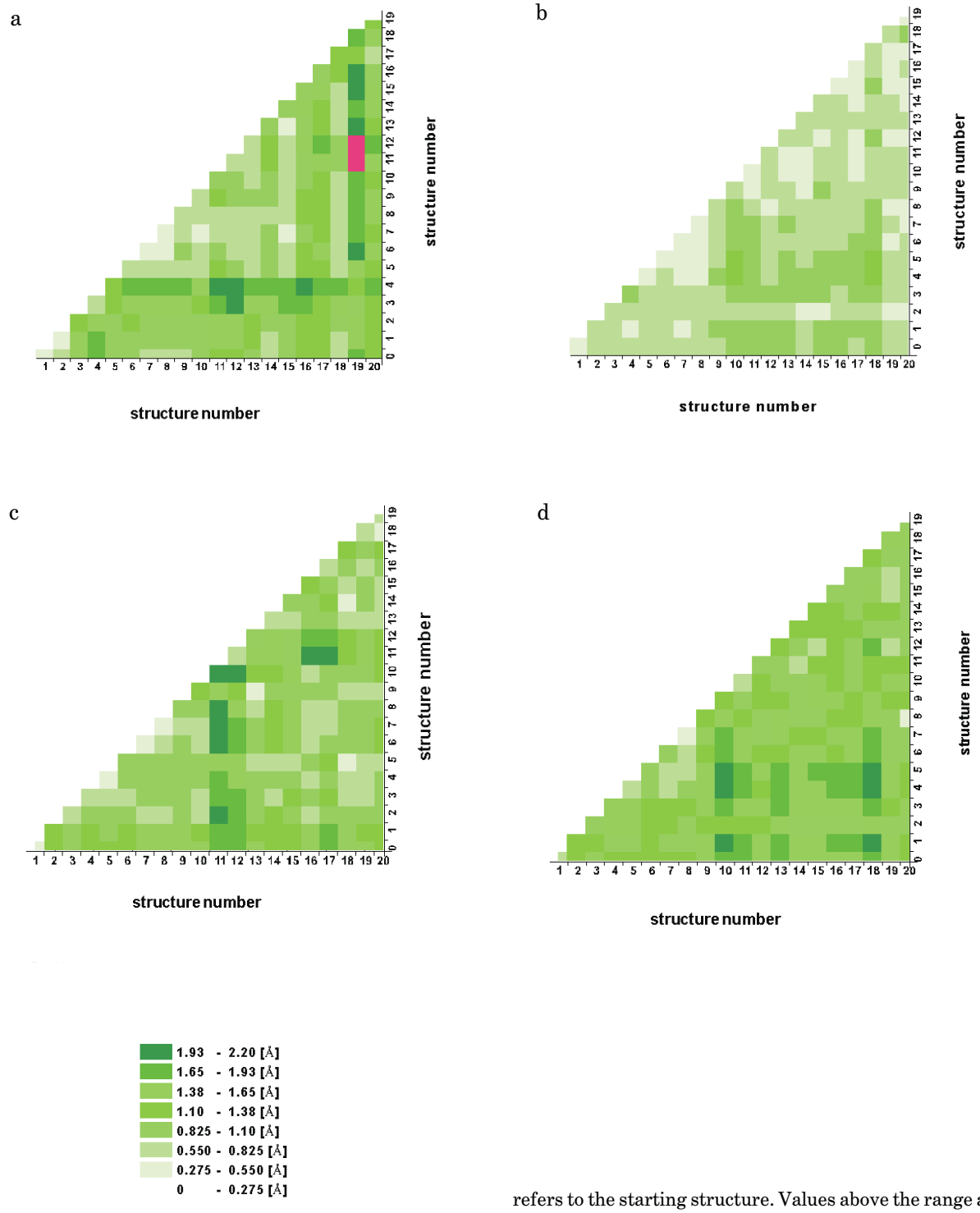

Figure 7. Colour representation of root mean square displacement (r.m.s.d.) matrices, calculated for all 20 optimised structures, obtained during simulated annealing (see 'Methods') of α_1-antitrypsin. The starting, optimised structures were also included.

Colour scale was applied to depict each value range (see legend). Tick labels denote structure numbers. Number '0' refers to the starting structure. Values above the range are coloured red. Each pair of matrices represents a comparison of r.m.s.d. values for the wild type (a, c) and the Z mutant (b, d). The r.m.s.d. values were calculated for C_α atoms. These values represent structural similarity of models; the darker the colour, the higher the r.m.s.d. value for a given pair of structures. The analysis shown in (a) and (b) was done for the chain comprising an upper part of the strand 3A and a part of the β-turn connected to strand s4C. It extends to the left of the molecule (view as in Fig. 6a). Figures (c) and (d) refer to the reactive loop, including the hinge region indicated in Fig. 6a.

the simulation, a new area in the local conformational space.

Diagrams in 7a, b refer to the region close the 'hinge' indicated in Fig. 6a. This fragment does not exhibit any defined tertiary structure but may be classified as a polypeptide chain having fairly well defined β conformation. In the wild type, the largest divergence is observed for the structures No. 5 and 19. In the mutant, distribution of r.m.s.d. values is more uniform, and the values do not exceed 1.38 Å. According to the diagrams, r.m.s.d. values between structures in the set 0–20 are lower in the mutant than in the wild type model. This indicates that, in this fragment, the Z mutation does not induce a more effective penetration of conformational space.

For structures No. 11 and 13 of the wild type, relatively large structural divergence around 2 Å is observed. The mutant model exhibits a larger divergence in this fragment of polypeptide chain and, a more uniform distribution of r.m.s.d. values than the wild type model. One may conclude that the exchange Glu342→Lys increases penetration of conformational space by the reactive loop. However, the phenomenon is weaker than one might expect.

Table 1. The r.m.s. values for selected sets of structures, generated during MD simulation of α_1-antitrypsin at 500 K.

Values for the wild type and the mutant are in the upper and lower part of the table, respectively. All r.m.s. values are in ångstroms.

Wild type / Z mutant	0 ps	50 ps	100 ps	150 ps	200 ps
0 ps	0	2.36	2.57	2.32	2.18
50 ps	2.03	0	1.54	1.39	1.85
100 ps	2.33	1.52	0	1.34	1.90
150 ps	2.18	1.49	1.35	0	1.59
200 ps	2.24	1.56	1.46	1.23	0

Secondary structure variation of optimised models

To identify changes in secondary structure of an optimised mutant model, analysis based on Kabsch and Sander classification was performed. It was analogous to that described above, but both the wild type and the mutant model were the most 'optimal' structures, i.e. taken after 170 and 140 ps of high temperature MD, respectively. The largest divergence is observed at the 'hinge' of the reactive loop, and starts from Ile340. Similarly to findings from the analysis of 'dynamical' models, a 4-residue bend is created in the mutant, while no ordered secondary structure is seen in the diagram for the wild type. Other major differences were approximately the same as those described above.

Within the reactive loop, no clearly defined elements of secondary structure were identified on the diagram. This is the case for the four modelled structures of α_1-antitrypsin, described in this paper (two 'dynamical' and two 'optimised'). Instead, we observe differences in backbone conformation of two fragments, one connecting the F helix and the other connecting the I helix to the A sheet. Most often the conformational variations between the models of the Z mutant and the wild type are the same for 'dynamical' and 'optimised' structures.

CONCLUDING REMARKS

The results obtained indicate that the Z mutation introduces local conformational changes in the region of the reactive loop, particularly at the 'hinge' close to residues No. 342 and 290. Moreover, even parts of the protein located far apart

from this region change their conformation upon mutation. r.m.s. differences between 'optimised' structures are comparable to an experimental error of X-ray determination of protein structures. These data, together with results of detailed analysis of the conformational searching process lead to the hypothesis that the Z mutation principally induces changes in dynamics of the protein. Although this theory based hypothesis does not contradict experimental results, further simulations are needed to verify this statement. Results that will be both quantitative and verifiable can be obtained by applying more accurate modelling methods (work currently in progress).

REFERENCES

1. Holaday, S.K., Martin, B.M., Fletcher, P.L. & Krishna, N.R. (2000) NMR solution structure of butantoxin. *Arch. Biochem. Biophys.* **379**, 18–27.
2. Gettins, P.G.W., Patston, P.A. & Olson, S.T. (1996) S*erpins: Structure, Function and Biology*; pp. 1, 111, 177. Chapman & Hall, R.G. Landes and Austin, Texas.
3. Parmar, J.S. & Lomas, D.A. (2000) α_1-Antitrypsin deficiency, the serpinopathies and conformational disease. *J. R. Coll. Physicians. Lond.* **34**, 295–300.
4. Elliott, P.R., Pei, X.Y., Dafforn, T.R. & Lomas, D.A. (2000) Topography of a 2.0 Å structure of α_1-antitrypsin reveals targets for rational drug design to prevent conformational disease. *Protein. Sci.* **9**, 1274–1281.
5. Lomas, D.A. (2000) Loop-sheet polymerization: The mechanism of α_1-antitrypsin deficiency. *Respir. Med.* **94**, S3–S6.
6. Sivasothy, P., Dafforn, T.R., Gettins, P.G. & Lomas, D.A. (2000) Pathogenic α_1-antitrypsin polymers are formed by reactive loop-β-sheet A linkage. *J. Biol. Chem.* **275**, 33663–33668.
7. Loebermann, H., Tokuoka, R., Deisenhofer, J. & Huber, R. (1984) Human α_1-proteinase inhibitor. Crystal structure analysis of two crystal modifications, molecular model and preliminary analysis of the implications for function. *J. Mol. Biol.* **177**, 531–556.
8. Elliott, P.R., Abrahams, J. & Lomas, D.A. (1998) Wild-type α_1-antitrypsin is in the canonical inhibitory conformation. *J. Mol. Biol.* **275**, 419–425.
9. Mahadeva, R., Chang, W.S., Dafforn, T.R., Oakley, D.J., Foreman, R.C., Calvin, J., Wight, D.G. & Lomas, D.A. (1999) Heteropolymerization of S, I, and Z α_1-antitrypsin and liver cirrhosis. *J. Clin. Invest.* **103**, 999–1006.
10. Elliott, P.R., Bilton, D. & Lomas, D.A. (1998) Lung polymers in Z α_1-antitrypsin deficiency-related emphysema. *Am. J. Respir. Cell. Mol. Biol.* **18**, 670–674.
11. Carrell, R.W., Lomas, D.A., Sidhar, S. & Foreman, R. (1996) α_1-Antitrypsin deficiency. A conformational disease. *Chest* **110**, 243S–247S.
12. Lomas, D.A., Evans, D.L., Finch, J.T. & Carrell, R.W. (1992) The mechanism of Z α_1-antitrypsin accumulation in the liver. *Nature* **357**, 605–607.
13. Yu, M., Lee, K.N. & Kim, J. (1995) The Z type variation of human α_1-antitrypsin causes a protein folding defect. *Nature Struct. Biol.* **2**, 363–367.
14. Lomas, D.A., Evans, D.L., Stone, S.R., Chang, W.S. & Carrell, R.W. (1993) Effect of the Z mutation on the physical and inhibitory properties of α_1-antitrypsin. *Biochemistry* **32**, 500–508.
15. Dunstone, M.A., Dai, W., Whisstock, J.C., Rossjohn, J., Pike, R.N., Feil, S.C., Le Bonniec, B.F., Parker, M.W. & Bottomley, S.P. (2000) Cleaved antitrypsin polymers at atomic resolution. *Protein Sci.* **9**, 417–420.
16. Huntington, J.A., Pannu, N.S., Hazes, B., Read, R.J., Lomas, D.A. & Carrell, R.W. (1999) A 2.6 Å structure of a serpin polymer and implications for conformational disease. *J. Mol. Biol.* **293**, 449–455.
17. Dafforn, T.R., Mahadeva, R., Elliott, P.R., Sivasothy, P. & Lomas, D.A. (1999) A Kinetic mechanism for the polymerization of α_1-antitrypsin. *J. Biol. Chem.* **274**, 9548–9555.
18. Koloczek, H., Banbula, A., Salvesen G.S. & Potempa, J. (1996) Serpin α_1-proteinase inhibitor probed by intrinsic tryptophan fluorescence spectroscopy. *Protein Sci.* **5**, 2226–2235.
19. Carrell, R.W., Stein, P.E., Fermi, G. & Wardell, M.R. (1994) Biological implications of a 3 Å structure of dimeric antithrombin. *Structure* **2**, 257–270.

20. Jorgensen, W.L. & Tirado-Rives, J. (1988) The OPLS potential functions for proteins. Energy minimizations for crystals of cyclic peptides and crambin. *J. Am. Chem. Soc.* **110**, 1657–1666.

21. Ryckaert, J.-P., Ciccotti G. & Berendsen, H.J.C. (1977) Numerical integration of the Cartesian equations of motion of a system with constraints: Molecular dynamics of n-alkanes. *J. Comp. Phys.* **23**, 327–341.

22. Berendsen, H.J.C., Postma, J.P.M., van Gunsteren, W.F., DiNola, A. & Haak, J.R. (1984) Molecular dynamics with coupling to an external bath. *J. Chem. Phys.* **81**, 3684–3690.

23. Pearlman, D.A., Case, D.A., Caldwell, J.C., Seibel, G.L., Singh, U.C., Weiner, P. & Kollman, P.A. (1991) *AMBER 4.0.* University of California, San Francisco.

24. Tejero, R., Bassolino-Klimas, D., Bruccoleri, R.E. & Montelione, G.T. (1996) Simulated annealing with restrained molecular dynamics using CONGEN. *Protein Sci.* **5**, 578–592.

25. Li, H., Tejero, R., Monleon, D., Bassolino- Klimas, D., Abate-Shen, C., Bruccoleri, R.E. & Montelione, G.T. (1997) Homology modeling using simulated annealing of restrained molecular dynamics and conformational search calculations with CONGEN. *Protein Sci.* **6**, 956–970.

26. *BIOSYM/MSI* (1997, 1998) Molecular Simulations, San Diego, California.

27. Kabsch, W. & Sander, Ch. (1983) Dictionary of protein secondary structure: Pattern recognition of hydrogen-bonded and geometrical features. *Biopolymers* **22**, 2577–2637.